Phosphotransfer Site of the Chemotaxis-Specific Protein Kinase CheA as Revealed by NMR†

Hongjun Zhou and Frederick W. Dahlquist*

Institute of Molecular Biology, University of Oregon, Eugene, Oregon 97403

Received July 9, 1996; Revised Manuscript Received September 9, 1996⊗

ABSTRACT: Bacterial chemotaxis involves autophosphorylation of a histidine kinase and transfer of the phosphoryl group to response regulators to control flagellar rotation and receptor adaptation. The phosphotransfer domain, $CheA_{1-134}$, of the chemotaxis-specific histidine autokinase CheA from *Escherichia coli* contains the site of phosphorylation, His48, and two other histidine residues, His26 and His67. Two-dimensional $^{1}H-^{15}N$ NMR techniques were applied to characterize the protonation states of these histidine residues and to evaluate the structural changes in the domain that occur upon phosphorylation of His48. The pK_a of His48 was determined to be 7.8 (in 50 mM $NaPO_4$ buffer at 30 °C). At high pH, its imidazole ring exists primarily as the normally unfavored $N^{\delta 1}H$ tautomer, suggesting hydrogen bond formation to the ring nitrogen atom(s) to stabilize this state. The pK_a values and predominant tautomeric states of the imidazole rings of His26 (p$K_a \sim 7.1$, $N^{\epsilon 2}H$ tautomer) and His67 (p$K_a \sim 6.5$, $N^{\delta 1}H$ tautomer) were also determined. His48 of $CheA_{1-134}$ and $CheA_{1-233}$ was phosphorylated by full-length CheA. The phosphorylation site was confirmed to be the $N^{\epsilon 2}$ position in the imidazole ring. Phosphorylation of His48 only results in small changes in the amide ^{1}H and ^{15}N chemical shifts of a few residues from helices B and C, suggesting that only very small changes in structure are associated with phosphorylation of the phosphotransfer domain of CheA. These residues occupy a small surface area of the helix bundle and form the active site of the protein. At the active site, in addition to His48, residues Gly52, His67, and Glu70 are conserved in the CheA homologous phosphotransfer domains from 10 different organisms. Sequence comparison of these CheA homologs suggest that the phosphotransfer domains likely fold in a similar helix−bundle structure and the structural features at the active site are well-conserved.

Escherichia coli responds to chemical stimuli by migrating toward favorable environmental conditions and away from harmful ones. This process involves the participation of several proteins in the chemotaxis system which use information from the receptors on the cell surface to ultimately control the sense of flagellar rotation [for reviews, see Stewart and Dahlquist (1987), Bourret et al. (1991), and Parkinson and Kofoid (1992)]. This signal transduction process requires specific phosphorylation and dephosphorylation reactions. CheA is a histidine autokinase that phosphorylates at His48 (Hess et al., 1988) located in the N-terminal phosphotransfer domain. The phosphoryl group is transferred to the response regulator proteins CheY (Hess et al., 1988; Stock et al., 1988a; Sanders et al., 1989) or CheB (Lupas & Stock, 1989; Ninfa et al., 1991). The phosphorylated form of CheY interacts with the flagellar switch complex to change the direction of rotation of the flagella (Barak & Eisenbach, 1992; Roman et al., 1992); the phosphorylated form of CheB has enhanced methylesterase activity which modulates the sensitivity of the receptor−CheW−CheA complex to extracellular stimuli (Simms et al., 1985; Lupas & Stock, 1989).

The autophosphorylation activity of CheA is modulated by the membrane-spanning receptors through the receptor−CheW−CheA complex (Gegner et al., 1992). The receptors bind and signal the presence of various chemoattractants and -repellents. In addition, the Tsr receptor appears to be involved in pH sensing (Slonczewski et al., 1982). It is also possible that internal pH is sensed directly by CheA. Conley et al. (1994) have demonstrated that CheA autokinase activity exhibits a bell-shaped dependence upon pH *in vitro* within the range of pH values from 6.5 to 10.0. This pH dependence suggests that a specific protonation state of the phospho-accepting histidine is required in the phosphotransfer reaction and that this in turn may serve as an effective internal pH sensor. By using two-dimensional (2D)[1] $^{1}H-^{15}N$ NMR techniques, we were able to directly examine the resonances from the imidazole rings of the phosphorylation site His48 and two other histidine residues, His26 and His67, and to determine their pK_a values and the predominant tautomeric states.

The global fold of the phosphotransfer domain ($CheA_{1-134}$) of CheA from *E. coli* is the first structure of such domains determined in the CheA family (Zhou et al., 1995). This domain consists of five helices which form a rigid and compact helix bundle. The phosphorylation site His48 in $CheA_{1-134}$ resides near the C terminus of helix B and at the interface of helices B and C. The imidazole ring is exposed to the solvent in the current structure, which was determined using a limited number of distance restraints. Backbone

† This work was supported by a grant from the National Institutes of Health (GM 33677 to F. W. D.).

* Author to whom correspondence should be addressed.

⊗ Abstract published in *Advance ACS Abstracts,* January 1, 1997.

[1] Abbreviations: NMR, nuclear magnetic resonance; HSMQC, heteronuclear single-multiple-quantum coherence; HMQC, heteronuclear multiple-quantum coherence; 2D, two-dimensional; TPPI, time-proportional phase incrementation; PTS, phosphoenolpyruvate:glycose phosphotransferase system.

S0006-2960(96)01663-7 CCC: $14.00

dynamics studies show that the structure around His48 is fairly rigid (Zhou et al., 1995), suggesting that structural changes upon phosphorylation of this residue are likely to be limited and localized. The phosphorylation position in the imidazole ring of His48 is cited in Stock et al. (1989) as the $N^{\epsilon 2}$ position without supporting evidence. By using 2D $^1H-^{15}N$ NMR spectroscopy, we have confirmed the site of phosphorylation in the imidazole ring of His48. The absence of large chemical shift changes in the amide $^1H-^{15}N$ resonances of $CheA_{1-134}$ and $CheA_{1-233}$ upon phosphorylation suggests that only localized and minor structural changes occur in these proteins upon phosphorylation.

We also have generalized the global fold and the structural features at the active site of the phosphotransfer domain of CheA from *E. coli* to the homologous domains from several other organisms. This shows that, in addition to His48, several other conserved residues, Gly52, His67, and Glu70, at the active site are likely important in establishing the proper tautomeric form of His48 in the resting enzyme and may direct positioning of the phosphoryl group.

MATERIALS AND METHODS

Sample Preparation. Expression and purification of uniformly ^{15}N-labeled $CheA_{1-134}$ and $CheA_{1-233}$ have been described previously (Swanson et al., 1993; Zhou et al., 1995, 1996). Protein samples were dialyzed against 50 mM $NaPO_4$ at pH 8.0 and concentrated to approximately 2 mM. D_2O (5%) and sodium azide (0.02%) were added to the NMR samples.

NMR Data Collection and Processing. All data reported in this paper were collected on a General Electric Omega 500 MHz spectrometer at 30 °C except as otherwise stated. The chemical shifts were set to an external proton reference of sodium 2,2-dimethyl-2-silapentane-5-sulfonate (DSS) at 0.0 ppm and an external nitrogen standard of $^{15}NH_4Cl$ at 24.93 ppm relative to $^{15}NH_3$. All data were processed using FELIX software (Hare Research, Biosym Technologies, San Diego, CA). In the pH titration experiments, 2D $^1H-^{15}N$ HSMQC (Zuiderweg, 1990) and 2D $^1H-^{15}N$ HMQC (Bax et al., 1990) spectra were recorded for $CheA_{1-134}$ at the following pH values: 5.3, 5.5, 5.9, 6.3, 6.5, 6.8, 6.9, 7.2, 7.5, 7.7, 7.8, 8.3, 8.8, and 9.2. The pH was adjusted by adding NaOH or HCl. The HSMQC experiments were used to detect pH-dependent chemical shift changes of the amides; the HMQC experiments were used to detect chemical shift changes with pH for the histidine rings. In the HSMQC experiments, water signal suppression was achieved by a 0.85 s weak proton presaturation; in the HMQC experiment, a 1−1 echo suppression was used (Bax et al., 1990), with a time delay set to achieve maximum proton excitation at 8.2 ppm. A delay of 26 ms was used to refocus the evolution arising from the coupling between the carbon-bound protons and the imidazole nitrogens. In all experiments, the proton frequency was set to the water proton frequency of 4.76 ppm. The ^{15}N excitation was set to 116 ppm in the HSMQC experiments and 180 ppm in the HMQC experiments. Quadrature detection in the ^{15}N dimension was achieved by the States−TPPI method (Marion et al., 1989). A total of 256 real t_1 (^{15}N) and 1024 complex t_2 (^1H) points were recorded for each spectrum. Eight or sixteen scans were used for each real t_1 (^{15}N) point. The spectral width in the ^1H dimension was set to 6666.7 Hz. The spectral width in the ^{15}N dimension was set to 1041.6 Hz in the HSMQC experiments and to 10 000 Hz in the HMQC experiments. 2D $^1H-^{15}N$ HSMQC and HMQC spectra were also collected for $CheA_{1-233}$ at pH 6.3, 7.5, 8.0, and 9.7, with the same experimental parameters as for $CheA_{1-134}$.

For the phosphorylation experiments, 1 mM $CheA_{1-134}$ or $CheA_{1-233}$ in 50 mM $NaPO_4$ was mixed with approximately 0.15 mM $CheA_{1-654}$, 10 mM ATP, 5 mM $MgCl_2$, 100 mM KCl, and 2 mM β-mercaptoethanol. The samples were equilibrated at pH 7.5 and room temperature for 20 min before being loaded into an NMR tube. 2D $^1H-^{15}N$ HMQC and HSMQC spectra were recorded with the nitrogen excitation frequency set in the amide and imidazole nitrogen regions, respectively. An HMQC-J spectrum (Kay & Bax, 1990) was recorded for a phosphorylated $CheA_{1-233}$ sample to detect changes of the $^3J_{HN\alpha}$ coupling constants.

Analysis of the pH Titration Data. The expected cross-peak patterns of the imidazole ring in the $^1H-^{15}N$ HMQC spectrum have been described in detail (van Dijk et al., 1992; Pelton et al., 1993). The imidazole ring can exist in three protonation states: one charged state and two neutral tautomers ($N^{\epsilon 2}H$ or $N^{\delta 1}H$) (Witanowski et al., 1972; Bachovchin, 1986). In general, with a proper refocusing delay in the pulse sequence (26 ms in our experiments), four $^1H-^{15}N$ correlation cross-peaks between either of the two imidazole nitrogens and either of the two carbon-bound ring protons can possibly be observed in the HMQC spectrum. The intensity and line width of these cross-peaks depend on pH, the through-bond coupling constants, the exchange rates between the three states, and the relaxation times of the ^1H and ^{15}N nuclei.

The chemical shift of a nitrogen nucleus strongly depends on its protonation state. For a protonated imidazole ^{15}N nucleus, the neutral (type α) and charged (type α^+) forms have shifts of 167.5 and 176.5 ppm, respectively, whereas the deprotonated ^{15}N (type β) has a shift of 249.5 ppm (Bachovchin, 1986; Pelton et al., 1993). It needs to be noted that our ^{15}N reference is that of Pelton et al. (1993) which is different from that of Bachovchin (1986). Depending on the exchange rates between the neutral states, several different situations might appear (van Dijk et al., 1992). Fast tautomerization between the neutral states is often observed. In this condition, the apparent ^{15}N chemical shifts are the fraction-weighted averages of those of the three pure states. At the low-pH limit, the observed chemical shifts are reduced to those of the pure protonated state; at the high-pH limit, these chemical shifts are the weighted average of the shifts of the neutral tautomers. When the chemical shifts of the protonated form and neutral forms are compared with model shift values, valuable information on the predominant tautomeric state of a histidine and possible hydrogen bond formation to the imidazole nitrogens can be obtained (Bachovchin, 1986).

The information concerning hydrogen bonding is obtained from either the chemical shift values of the nitrogens or the derived tautomer fractions (Bachovchin, 1986). Hydrogen bonding produces changes in the ^{15}N chemical shifts resembling those produced by protonation/deprotonation but having a much smaller magnitude (Schuster & Roberts, 1979). A nitrogen acting as a hydrogen donor shows a smaller chemical shift; a nitrogen acting as a hydrogen acceptor shows a larger chemical shift. The amplitude of the change, up to 10 ppm, has been considered to reflect the

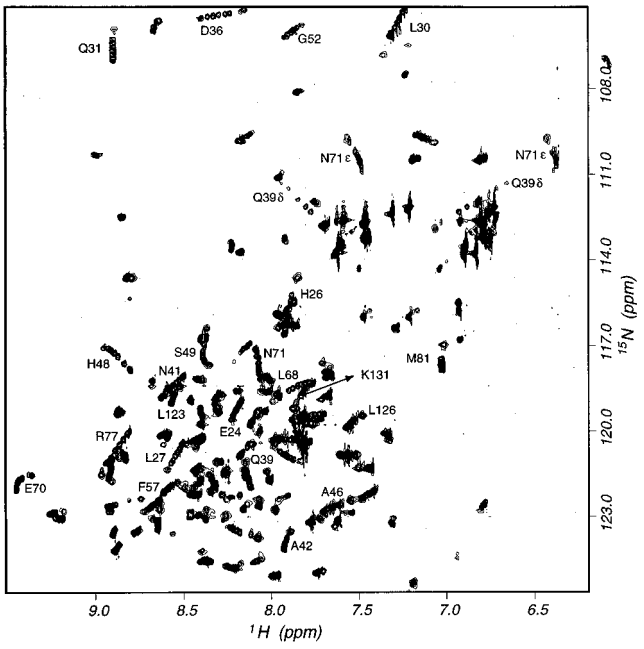

FIGURE 1: Overlay of 13 $^1H-^{15}N$ HSMQC spectra from $CheA_{1-134}$ taken at pH 5.3, 5.5, 5.9, 6.3, 6.5, 6.7, 6.9, 7.2, 7.7, 7.8, 8.3, 8.8, and 9.2.

strength of the hydrogen bond (van Dijk et al., 1990). It should be noted that this comparison depends on the model chemical shifts used which were derived from NMR studies of model compounds and is complicated by the specific structural environment of a histidine in a protein. The other indication of hydrogen bond formation is the observed predominance of the $N^{\delta 1}H$ tautomer over the normally favored $N^{\epsilon 2}H$ tautomer (Reynolds & Tzeng, 1976; Bachovchin, 1986).

To extract the apparent pK_a values of the imidazole rings or the backbone amides, the chemical shifts at various pH values were least-squares fit by the Henderson−Hasselbach equation:

$$\delta_{obs} = \delta_1 10^{-pH}/(10^{-pH} + 10^{-pK_a}) + \delta_2 10^{-pK_a}/(10^{-pH} + 10^{-pK_a}) \quad (1)$$

where δ_1 and δ_2 are the chemical shifts at the low- and high-pH limits, respectively. This equation gives the observed chemical shift, δ_{obs}, as a weighted average of the limiting values δ_1 and δ_2. In this model, fast exchange between the states at low- or high-pH extremes is assumed. The least-squares fit was made using the program KaleidaGraph (Abelbeck Software).

RESULTS

The phosphotransfer domain, $CheA_{1-134}$, contains three histidine residues: His26, His48, and His67. To assign the imidazole resonances to specific histidines, we have compared the apparent pK_a values derived from the observed chemical shift changes of the backbone amide ^1H and/or ^{15}N nuclei with those of the imidazole rings. The assignments of His48 and His67 were confirmed in the phosphorylation experiments.

The chemical shifts of some of the backbone amide ^1H and ^{15}N nuclei of $CheA_{1-134}$ show a striking pH dependence. These data are shown in Figure 1 as a superposition of the $^1H-^{15}N$ correlation spectra of fully ^{15}N-labeled $CheA_{1-134}$ taken at several pH values. Those residues that exhibit the largest pH-dependent chemical shift changes are primarily histidine residues and their immediate neighbors. Most resonances fall along straight lines in these two-dimensional spectra between the positions observed at the most acidic and most basic conditions. This behavior is consistent with fast exchange between two states which are pure states at low- and high-pH extremes, respectively. Under the assumption of fast exchange between the two states and using eq 1, we were able to fit the chemical shifts as functions of pH values for most of these amide protons or nitrogens, as shown in Figure 2.

The apparent pK_a values extracted by observing the amide resonances of the histidines and their neighbors are similar to those we observe for the resonances of the imidazole rings. Additionally, the pH-dependent chemical shift changes of these amides appear to be localized and limited. Therefore, the chemical shift changes observed appear to arise primarily from changes in electronic induction effects on the amides in response to changes in protonation states of nearby imidazole rings. For those titration curves that do not have simple Henderson−Hasselbach behavior, multiple titrating groups or local structural adjustments in response to pH changes may contribute greatly to the chemical shift changes (Forman-Kay et al., 1992).

pH Titration of the Histidine Residues. Three histidines in $CheA_{1-134}$ present three sets of cross-peaks from the imidazole rings. Figure 3 shows a portion of an $^1H-^{15}N$ HMQC spectrum labeled with the assignments of the imidazole resonances.

His48. His48 is the site of autophosphorylation of CheA (Hess et al., 1988). The pH dependence of the imidazole ^1H and ^{15}N shifts for unphosphorylated His48 is shown in Figure 4. The chemical shifts of the resonances from the imidazole ring were pH-dependent, and a single averaged resonance was observed for each $^{15}N-CH$ pair during the complete titration course. The pK_a value of the imidazole ring was determined to be 7.8 using eq 1. The assignment of this residue was based on similar pK_a values reported by the backbone amides of His48, Ser49, and Ala47 and was confirmed by the significant changes of the imidazole resonances upon phosphorylation of $CheA_{1-134}$.

For protonated His48, the $N^{\epsilon 2}$ shift of 175.6 ppm is close to the expected 176.5 ppm for a charged imidazole nitrogen, indicating no hydrogen bond formation to this nitrogen. The $N^{\delta 1}$ chemical shift of 185.9 ppm, however, is 9.4 ppm higher than expected, indicating that $N^{\delta 1}H$ acts as a hydrogen bond donor. At high pH, $N^{\epsilon 2}$ and $N^{\delta 1}$ resonate at 224.4 and 192.5 ppm, respectively. The larger shift of $N^{\epsilon 2}$ indicates that the $N^{\delta 1}H$ tautomer is dominant. Since the $N^{\delta 1}H$ tautomer is not the normally favored neutral state, this tautomer is likely stabilized by hydrogen bonding or other interactions with the rest of the protein.

The ^{15}N chemical shifts of the neutral states can be explained by fast equilibration of the two tautomers. The fraction of each tautomer present at high pH can be estimated by comparing the observed chemical shifts of the imidazole nitrogens with model shift values using eq 2 and 3:

$$167.5x + 249.5y = 192.5 \quad (2)$$

$$249.5x + 167.5y = 224.4 \quad (3)$$

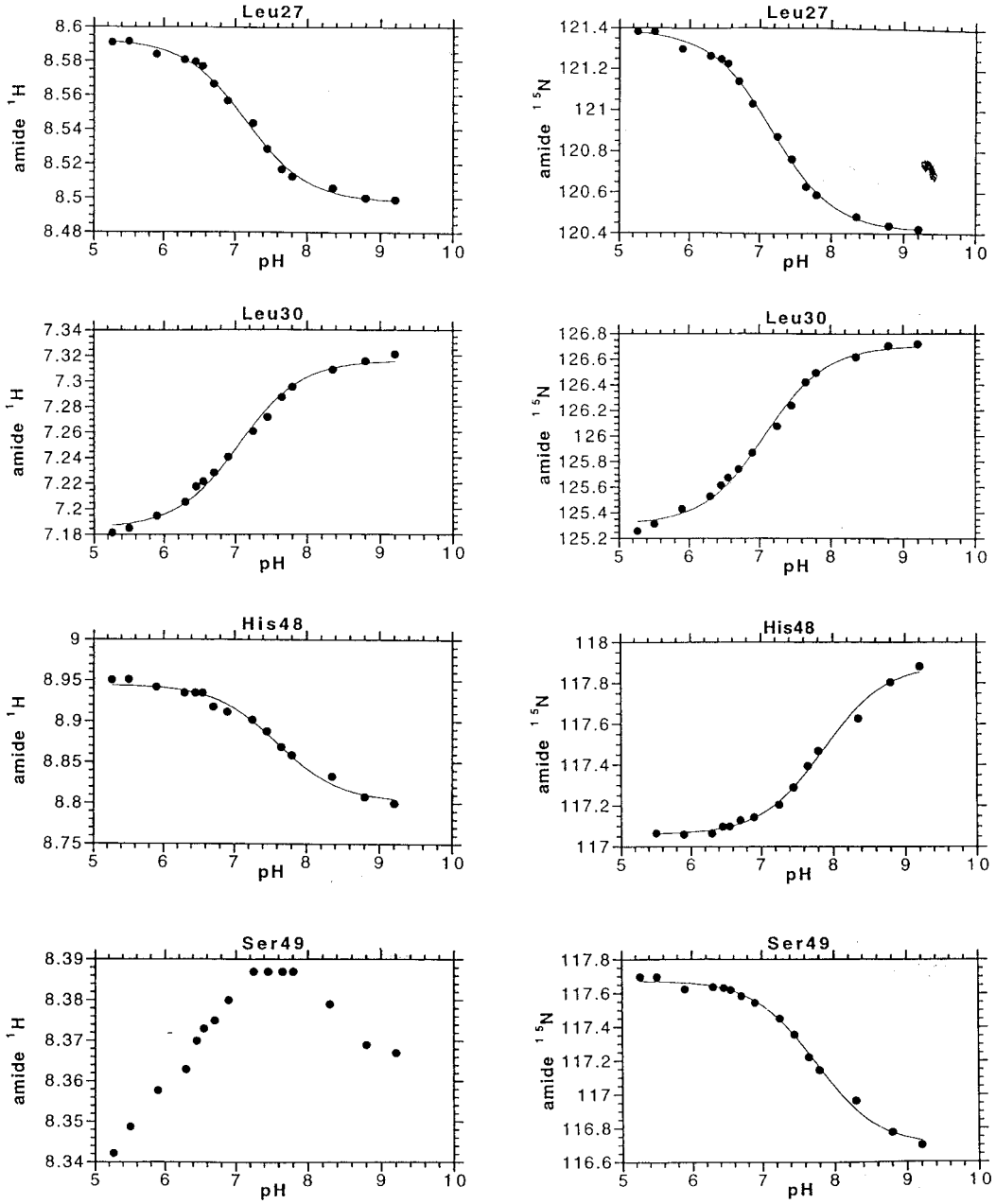

FIGURE 2: Selected plots of backbone amide chemical shifts as functions of pH. The solid line is the fit of the data points using eq 1. The derived pK_a values are reported in Table 1.

where x and y are the fractions of the $N^{\delta 1}H$ and $N^{\epsilon 2}H$ tautomers, respectively. Note that the model shifts on the left-hand sides of eqs 2 and 3 are the values for non-hydrogen-bonded nitrogens. Solving these equations for the two independent unknowns gives an x of 0.695, a y of 0.305, and an $N^{\delta 1}H/N^{\epsilon 2}H$ tautomeric ratio of 2.3/1. Remarkably, the sum of the independent values of x and y gives the ideal sum of unity. The average of the two nitrogen shifts is also nearly equal to the expected value of 208.5 ppm. These results are consistent with our basic assumptions, indicating the chemical shifts at high pH can be explained by fast tautomerization alone. This seems to contradict the idea of a single hydrogen bond formed to the imidazole ring. A single hydrogen bond would cause an ~10 ppm change in one of the model shift values in eqs 2 and 3, yielding an $x + y$ value away from the ideal value of 1 and an average nitrogen chemical shift approximately 5 ppm higher than expected. However, it is clear that reasonable but different tautomer fractions and the normal average chemical shift can still be obtained if both nitrogens participate in hydrogen bonds which cause opposite changes of the two model chemical shifts. Since hydrogen bonding alone cannot explain the large difference (>20 ppm) between the nitrogen shifts observed and the model shifts of pure type α or β nitrogens, fast tautomerization as well as hydrogen bonding involving both nitrogens seem to be required to explain the situation. While $N^{\epsilon 2}$ may be hydrogen-bonded only in the neutral forms, $N^{\delta 1}H$ is likely hydrogen-bonded at all pH values examined.

From the titration curve of His48, it is clear that the transition from the charged form to neutral forms of the imidazole ring is primarily associated with the deprotonation of $N^{\epsilon 2}H$. The flat titration curve for $N^{\delta 1}$ indicates that this atom is strongly protected from deprotonation. Hydrogen bonding to both nitrogens at high pH would require that $N^{\delta 1}H$ act primarily as a hydrogen donor and $N^{\epsilon 2}$ act primarily as

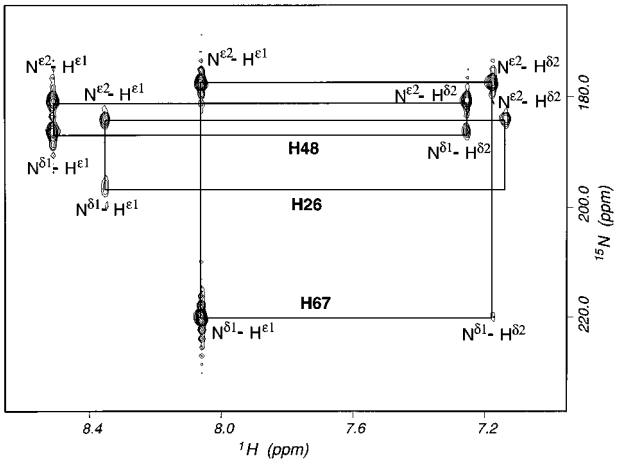

FIGURE 3: Selected portion of an $^{1}H-^{15}N$ HMQC spectrum from $CheA_{1-134}$ taken at pH 6.9 labeled with the assignments of the imidazole resonances from the histidine residues.

a hydrogen acceptor. Since fast tautomerization is also underway, the two nitrogens might exchange hydrogen bond partners through rapid ring rotation.

His26. The pK_a value of His26 was determined to be 7.1 (Figure 4). The residue-specific assignment was based on similar pK_a values reported for the amide protons and/or nitrogens of Glu24, His26, Leu27, Val29, and Leu30 (Table 1). The titration of the imidazole ring of His26 is not complete because the imidazole cross-peaks broadened and disappeared at pHs above 7.0 due to exchange processes.

At low pH, the $N^{\epsilon 2}$ and $N^{\delta 1}$ nitrogens shifts are 181.0 and 177.6 ppm, respectively. These values suggest no significant hydrogen bond formation to the $N^{\delta 1}$ nitrogen and weak hydrogen bond formation to the N^{e2} nitrogen. At high pH, $N^{\delta 1}$ has a much larger chemical shift than $N^{\epsilon 2}$, indicating that the $N^{\epsilon 2}H$ tautomer is dominant. Though the possibility of hydrogen bond formation at high pH cannot be evaluated, theoretically extracted limiting chemical shifts for the two nitrogens give an average of 207.2 ppm at the high-pH limit. This value is close to the expected 208.5 ppm. The $N^{\epsilon 2}H/N^{\delta 1}H$ ratio was calculated to be roughly 2/1. The nearly normal tautomeric ratio and average nitrogen chemical shift of the neutral states suggest no significant hydrogen bond formation to the imidazole ring.

Table 1: Apparent pK_a Values of Some of the Amide Protons and Nitrogens

	(N)H	N(H)		(N)H	N(H)
E24	7.26	7.22	S49		7.77
H26		7.12	I50		6.90
L27	7.11	7.15	K51	7.18	7.34
V29	7.04	7.11	T65	6.99	6.94
L30	7.20	7.19	T66		7.55
D36	7.12	7.04	H67		6.40
Q39	7.24	7.03	L68	7.00	6.44
N41	7.19	7.21	E70	6.43	7.66
A42		6.88	N71	7.93	7.71
I43	7.06	7.36	R77	6.89	7.28
A46	7.04	7.02	E93	7.13	
A47	7.66		L123	6.91	6.95
H48	7.67	7.88	L126	6.75	7.00

His67. While the carbon-bound ring protons and the imidazole nitrogens of His48 and His26 have similar pK_a values for each histidine, the apparent pK_a values reported for these nuclei are significantly different for His67. The $C^{\epsilon 1}H/C^{\delta 2}H$ protons and $N^{\epsilon 2}$ have pK_a values of ~6.5, whereas $N^{\delta 1}$ has a pK_a of ~7.4 (Figure 4). The chemical shift of $N^{\delta 1}$ is possibly affected by a nearby titrating group with a high pK_a value in a manner similar to the interactions

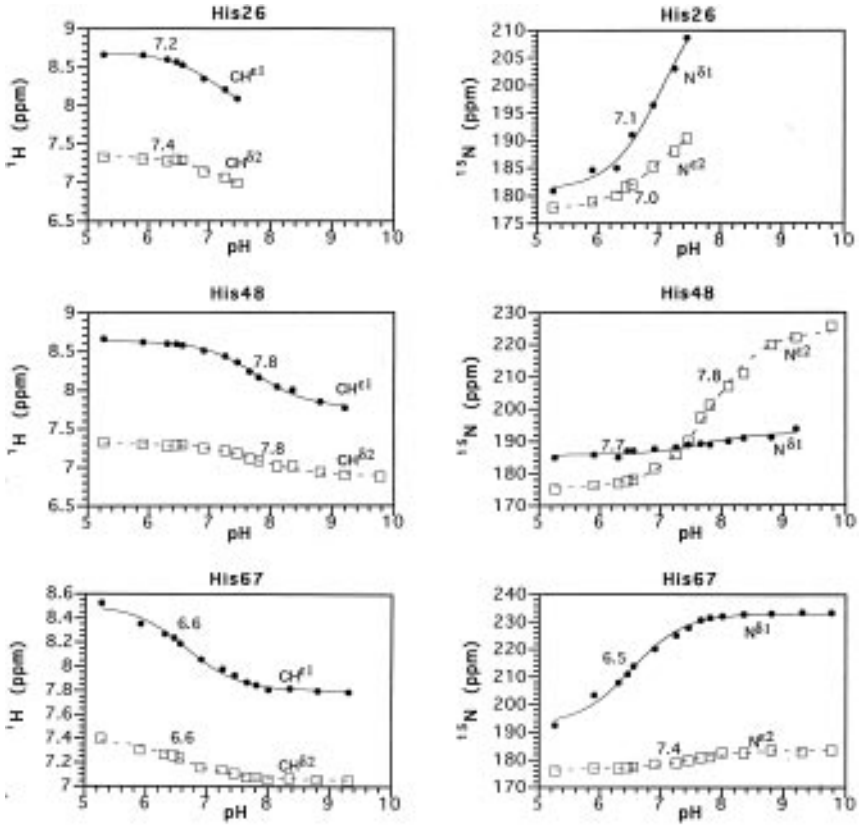

FIGURE 4: Chemical shifts of the imidazole ^{1}H and ^{15}N nuclei of His26 (top), His48 (middle), and His67 (bottom) as functions of pH. The solid or dashed line is the fit of the data points using eq 1. The derived pK_a value is shown for each curve.

between the backbone amides and nearby imidazole rings during the titration. The assignment of the imidazole resonances to His67 was based on the pK_a values of ~6.4 reported for the amide nitrogens of His67 and Leu68.

At low pH, the $N^{\epsilon 2}$ chemical shift, 176.6 ppm, is close to the expected 176.5 ppm, indicating no hydrogen bond formation to this atom. An accurate shift value for $N^{\delta 1}$ at low pH cannot be determined since the protein started to precipitate at pH <5. The calculated $N^{\delta 1}$ chemical shift of 192.6 ppm at the low-pH limit is much larger than the expected 176.5 ppm. However, the actual shift value of this nitrogen might be lower than 192.6 ppm if data at pH <5 are available. At high pH, $N^{\epsilon 2}$ and $N^{\delta 1}$ have shifts of 183.6 and 233.2 ppm, respectively. The average of these values is 208.4 ppm, close to the expected 208.5 ppm. At high pH, the histidine exists primarily in the $N^{\epsilon 2}H$ state. The $N^{\epsilon 2}H/N^{\delta 1}H$ ratio is 4/1, as calculated from $N^{\epsilon 2}$ and $N^{\delta 1}$ chemical shifts. For the neutral states, there is no indication of significant protein structure−dependent hydrogen bond formation.

pH Dependence of the Chemical Shifts of the Backbone Amides and Side Chain NH_2 Groups. Figure 1 shows an overlay of 13 $^1H-^{15}N$ correlation spectra from $CheA_{1-134}$ taken at pHs from 5.26 to 9.2. The chemical shifts of some of the amide protons and nitrogens are obviously sensitive to pH changes. The apparent pK_a values seen for those backbone amides with relatively large total chemical shift changes are summarized in Table 1. As discussed above, the correlations between the apparent pK_a values of the amides and those of nearby imidazole rings have aided in the assignments of the imidazole resonances to specific histidines.

The NH_2 groups of Gln39 and Asn71 also have apparent pK_a values which are close to those of nearby His26 and His67, respectively. Gln39 resides near the N terminus of helix B, which is proximal to His26 near the C terminus of helix A. The two NH_2 protons of Gln39 have apparent pK_a values of 7.1, and the NH_2 nitrogen has a pK_a value of 7.0. These values are equal or close to the pK_a value of 7.1 seen for the imidazole ring of His26. One of the NH_2 protons of Asn71 has a pK_a value of 6.6, while the other exhibited a more complex pH dependence (data not shown). This dependence indicates possible involvement of two ionizable groups or two states of conformation at low and high pH. However, the titration curve of the NH_2 nitrogen of Asn71 shows a smooth transition with a pK_a of 6.9. The different titration properties of these atoms may result from different local environments surrounding the NH_2 protons or a combination of local ionization and more distant conformational effects.

Phosphorylation of $CheA_{1-134}$ and $CheA_{1-233}$. $CheA_{1-134}$ and $CheA_{1-233}$ were phosphorylated by full-length CheA in the presence of ATP and Mg^{2+}. Figure 6 shows an $^1H-^{15}N$ HSQC spectrum from a partially phosphorylated $CheA_{1-134}$ sample. Two sets of cross-peaks appear in this spectrum, one from the unphosphorylated protein and the other from the phosphorylated protein. The appearance of isolated peaks from both forms of protein indicates that these forms interconvert slowly. The chemical shift changes of the phosphotransfer domain in $CheA_{1-233}$ upon phosphorylation of His48 are essentially the same as those for $CheA_{1-134}$ (data not shown). The cross-peaks from the CheY-binding domain were not detected to have significant changes upon phosphorylation of His48, indicating that this region does not interact with the phosphorylated phosphotransfer domain. In other experiments, the $CheA_{1-134}$ and $CheA_{1-233}$ samples were nearly fully phosphorylated, yielding peaks only from phosphorylated proteins (data not shown).

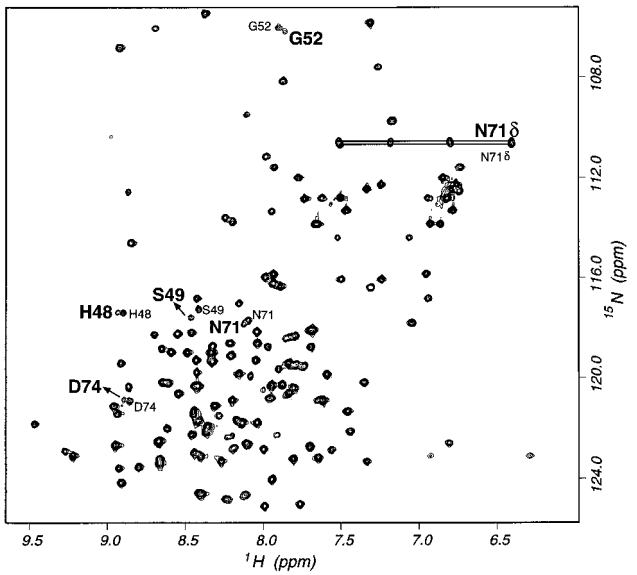

FIGURE 5: $^1H-^{15}N$ HSQC spectrum from a partially phosphorylated $CheA_{1-134}$ sample at pH 7.5 and 30 °C. Bold and large letters denote resonances from the phosphorylated form of the protein. Plain and small letters denote resonances from the unphosphorylated form of the protein. Only residues with detectable chemical shift changes after the phosphorylation are labeled. Straight lines indicate the resonances from the side chain NH_2 group of Asn71.

A few residues exhibit small but observable amide chemical shift changes upon phosphorylation of His48 (Figure 5). These residues are His48, Ser49, and Gly52 from helix B and Asn71 and Asp74 from helix C. The peaks from the side chain NH_2 group of Asn71 also show slight changes. These backbone and side chain chemical shift changes are probably caused by local structural changes or changes in chemical or electronic environments associated with phosphorylation of His48. We also looked for changes in the coupling constants upon phosphorylation as a probe of structural changes. The coupling constant $^3J_{HN\alpha}$ between the backbone amide proton and the $C^{\alpha}H$ proton is related to the backbone dihedral angle ϕ according to the Karplus equation. An $^1H-^{15}N$ HMQC-J experiment recorded on a $CheA_{1-233}$ sample shows no observable differences in $^3J_{HN\alpha}$ values between unphosphorylated and phosphorylated proteins (data not shown), suggesting the backbone conformation remains nearly identical in both forms of the protein. Therefore, changes in the side chain conformation or electronic shielding effect caused by the addition of the phosphate are likely responsible for the chemical shift changes observed.

For the imidazole ring of His48, cross-peak changes for the ring protons and nitrogens were observed when His48 was phosphorylated (Figure 6). Upon phosphorylation, $N^{\epsilon 2}$ of this histidine exhibits a chemical shift change of ~10 ppm while $N^{\delta 1}$ only shows an ~1 ppm change. Since the $N^{\delta 1}H$ form is predominant at neutral conditions, phosphorylation at $N^{\delta 1}H$ would deprotonate this nitrogen and cause a much larger chemical shift change at this position. Therefore, these results indicate that $N^{\epsilon 2}$ of His48 is the site of phosphorylation (Figure 7).

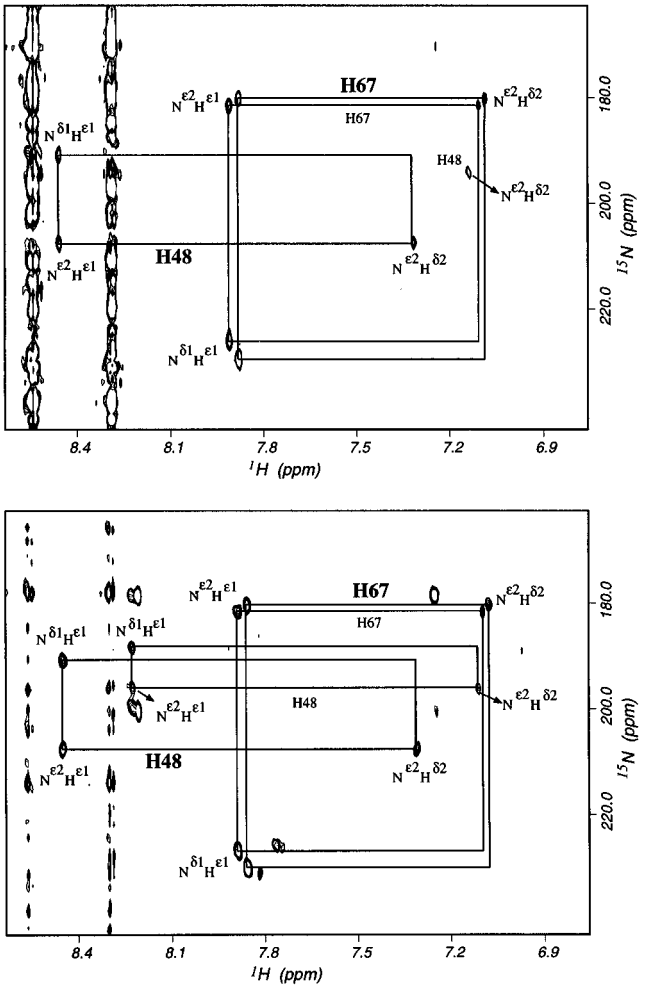

FIGURE 6: $^1H-^{15}N$ HMQC spectra at pH 7.5 and 30 °C showing the changes of the imidazole resonances upon phosphorylation of $CheA_{1-134}$ (top) and $CheA_{1-233}$ (bottom). Bold and big letters denote the peak sets from the phosphorylated form of the protein; plain letters denote peak sets from the unphosphorylated form of the protein.

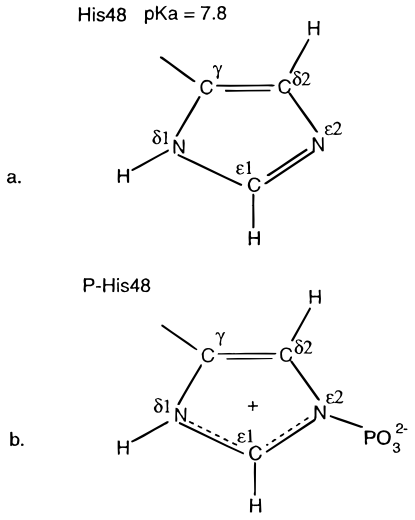

FIGURE 7: Predominant tautomeric state of His48 (a) and the phosphorylation position in the imidazole ring (b).

The small chemical shift change of His48 $N^{\delta 1}$ upon phosphorylation indicates this nitrogen remains protonated in the phosphoimidazole ring. The observed chemical shift of the phospho-$N^{\epsilon 2}$, 208.2 ppm, is between the expected 202.1 and 209.6 ppm values for phospho-^{15}N in neutral and charged phosphoimidazole rings, respectively (Pelton et al., 1993). Fast exchange between the predominant charged state and a slight amount of neutral form of the phosphohistidine ring explains the deviation of the phospho-$N^{\epsilon 2}$ shift from those of the pure states. According to the phospho-$N^{\epsilon 2}$ shift observed, the ratio of the neutral to charged forms of phosphoimidazole rings is roughly 1/4.3 at pH 7.5. $N^{\delta 1}$ of phosphorylated His48 exhibits a chemical shift of 192.8 ppm at this pH, which is between the chemical shifts of 174.4 and 244.4 ppm for protonated and deprotonated nitrogens, respectively, in a phosphoimidazole ring. A calculation similar to that for His48 $N^{\epsilon 2}$ yields a tautomeric ratio of 1/3.6 for the neutral and charged states of phosphorylated His48, consistent with the value from the $N^{\epsilon 2}$ shift. Although the pK_a value of phosphorylated His48 has not been determined by observing spectra as a function of pH, the predominance of the charged form at the experimental pH suggests that its pK_a is likely higher than 8.0.

The imidazole cross-peaks of His67 were also affected by phosphorylation of His48 (Figure 6). Phosphorylation of $CheA_{1-134}$ or $CheA_{1-233}$ resulted in two sets of nearby cross-peaks for the imidazole resonances of His67. These changes indicate that the imidazole ring of His67 is proximal to and possibly is involved in direct interactions with the imidazole ring of His48 and/or the phosphate. His26 resonances were not observed at pH 7.5 for both unphosphorylated and phosphorylated proteins.

The stability of the phosphorylated proteins varied significantly at different experimental conditions, although in all cases, the patterns of chemical shift changes upon phosphorylation were the same. At room temperature or 30 °C, the phosphorylated protein usually dephosphorylated in several hours in the original buffer, as judged by the reduction in the peak intensities for the phosphorylated form of proteins. When a partially phosphorylated $CheA_{1-134}$ sample was dialyzed against $NaPO_4$ buffer at pH 7.5 to remove the ATP, Mg^{2+}, and a small amount of ADP and stored at 4 °C, the protein stayed phosphorylated for several weeks. In one case, a nearly completely phosphorylated $CheA_{1-233}$ sample dephosphorylated slowly in 3 days at 30 °C. What causes these differences in the long term is not clear. However, it is clear that the phosphorylated forms of these domains are quite stable by themselves.

Sequence Comparison and Structural Similarity of the CheA Homologs. The three histidines in $CheA_{1-134}$ are readily titratable, consistent with their solvent-accessible positions in the global fold of $CheA_{1-134}$ (Zhou et al., 1995). Those residues that are affected by either titration or phosphorylation of His48, mostly polar or charged, are localized in a small region on one surface of the protein at the interface of helices B and C (Figure 8). Although the side chain orientations of these residues are not well-defined in the current structure, all of them are in the vicinity of the phosphorylation site. Interactions between these residues and His48, the active sites in the kinase domain of CheA, or the phosphate group might be critical to the phosphotransfer reaction and the stabilization of the phosphoimidazole in direct or indirect manners.

In order to investigate the conserved structural features of the phosphotransfer domains of the CheA proteins, we performed a computer search of protein sequence data bases and compared the CheA homologous sequences from 10 different organisms (Figure 9). Each of these CheA ho-

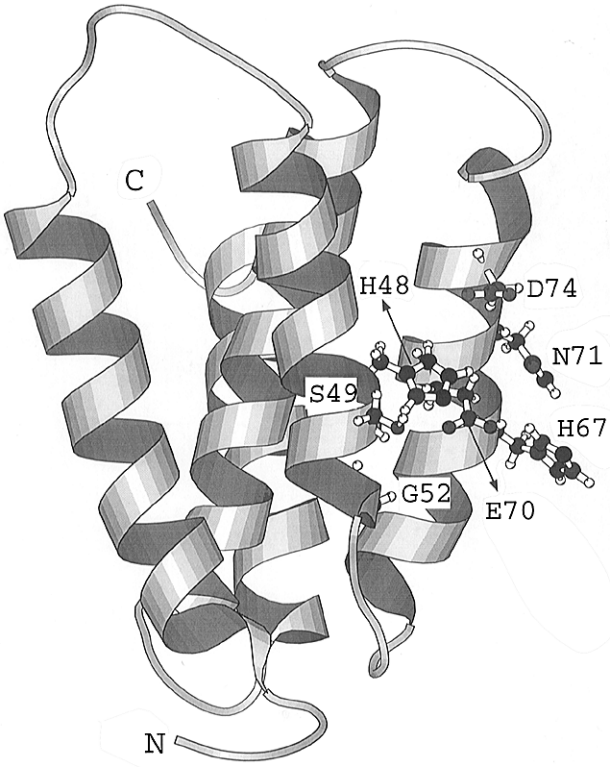

FIGURE 8: Ribbon diagram of $CheA_{1-134}$ (Zhou et al., 1995) showing the residues that are affected by titration of phosphorylation of His48.

mologs appears to have a separate phosphotransfer domain in the N-terminal region and a conserved kinase domain in the central region. Other regions may differ significantly. For example, FrzE, the CheA homolog from *Myxococcus xanthus*, does not have the CheY-binding region of *E. coli* CheA (Parkinson & Kofoid, 1992); instead, a region homologous to CheY is attached at the C terminus, and the region between P1 and the kinase domain is replaced by a long proline-alanine-rich sequence.

With the knowledge from previous structural, dynamic, and functional studies of *E. coli* CheA, we looked for structural features that are most conserved among the phosphotransfer domains of the CheA proteins and asked (1) if these homologous domains fold in the same fashion, that is in a helix−bundle, (2) if the structural features at the active site are conserved, and (3) if there is a fifth helix in other CheA proteins.

Figure 9 shows the sequence alignments of the N-terminal regions of the 10 CheA homologs. Sequence identity is localized primarily in the regions corresponding to helices A−C in *E. coli* CheA and the turns joining the three helices. Amino acid sequence similarity is primarily localized in the N-terminal four helical regions. The sequences corresponding to C-terminal helix E of *E. coli* CheA display the least similarity. The turn regions, which mostly contain proline or glycine residues, seem to be roughly at the same positions.

To ask if the putative helical regions have hydrophobic and hydrophilic surfaces similar to those of $CheA_{1-134}$, we placed the residues in the helical regions of five proteins onto a helical wheel diagram (Figure 10). It is clear that the distributions of hydrophobic and hydrophilic residues are quite similar for the five proteins, especially in helices A−C. Hydrophobic residues are mostly buried, while the residues on the surface are mostly charged or polar residues. In some proteins, helix E seems to be short or in a completely different structure. This seems to be consistent with the apparent variations in size and the pattern of the hydrophobic surface of helix D. Previous structural studies of *E. coli* CheA suggest that helix E interacts primarily with helix D (Zhou et al., 1995, 1996). In some CheA proteins, helix D may have an extended hydrophobic surface in order to interact with the "extra" helix E; in others, helix E is absent or short, and helix D has a smaller hydrophobic surface. while the hydrophobicity repeat in helix D is similar for most sequences, this helix may be curved or may break into two helices. This is suggested by the appearance of glycines near the middle of helix D in several sequences.

Another important finding from the sequence alignment is that the structural features at the active site seem to be conserved. Sequence homology is the highest in the region corresponding to helices B and C which carry nearly all the active site residues. Among the residues that are affected by titration or phosphorylation of His48 in *E. coli* CheA, residues Gly52, His67, and Glu70 are totally conserved. The phosphorylation site histidine is followed by either a serine or a threonine. This suggests that the hydroxyl group of the serine or threonine plays an important structural or functional role, consistent with previous observations. Mutation of Ser49 to an alanine in *E. coli* CheA significantly decreased the autophosphorylating activity (Hess et al., 1988). Mutation of Ser49 to a threonine led to the retention of a significant degree of CheA autokinase activity. Three positively charged residues from helix B or C and in the vicinity of the phosphorylation site, Arg45, Lys51, and Arg77, are highly conserved. These charged residues may play a role in stabilizing the phosphohistidine through electrostatic interactions. Lys51 and Arg77 are at the C termini of helices B and C, respectively. These residues may also stabilize the helical structure of the protein by interacting with the effective negative charges of the helix dipoles. Two glycines (Gly52 and Gly58) in the turn joining helices B and C are highly conserved. This turn region was observed to form a well-defined structure and may play an important functional role. Interestingly, another histidine at the active site, His67, is totally conserved. Its structural or functional role may resemble that of the extra histidine in III^{Glc} in the PTS (Pelton et al., 1993).

Overall, the sequence comparison indicates that the N-terminal approximately 80 residues likely form similar helical structures with similar turns. The structures in helix D and especially helix E may differ between the CheA homologs. It appears that having the phosphorylation histidine reside at the outer interface of two helices is a common feature of the kinase CheA. The high sequence identity at the active site indicates that the structural features are highly conserved at this site among the CheA homologs.

DISCUSSION

Conley et al. (1994) observed that the CheA autokinase activity exhibits a bell-shaped dependence on pH *in vitro*, with the maximum activity at pH 8.5. Two titratable groups were proposed to explain this pH dependence. For the phosphotransfer to proceed, one group with a pK_a of 8.1 needs to be deprotonated and the other group with a pK_a of 8.9 needs to be protonated. Our studies show that the site of phosphorylation, His48, has a pK_a of 7.8 and is very likely

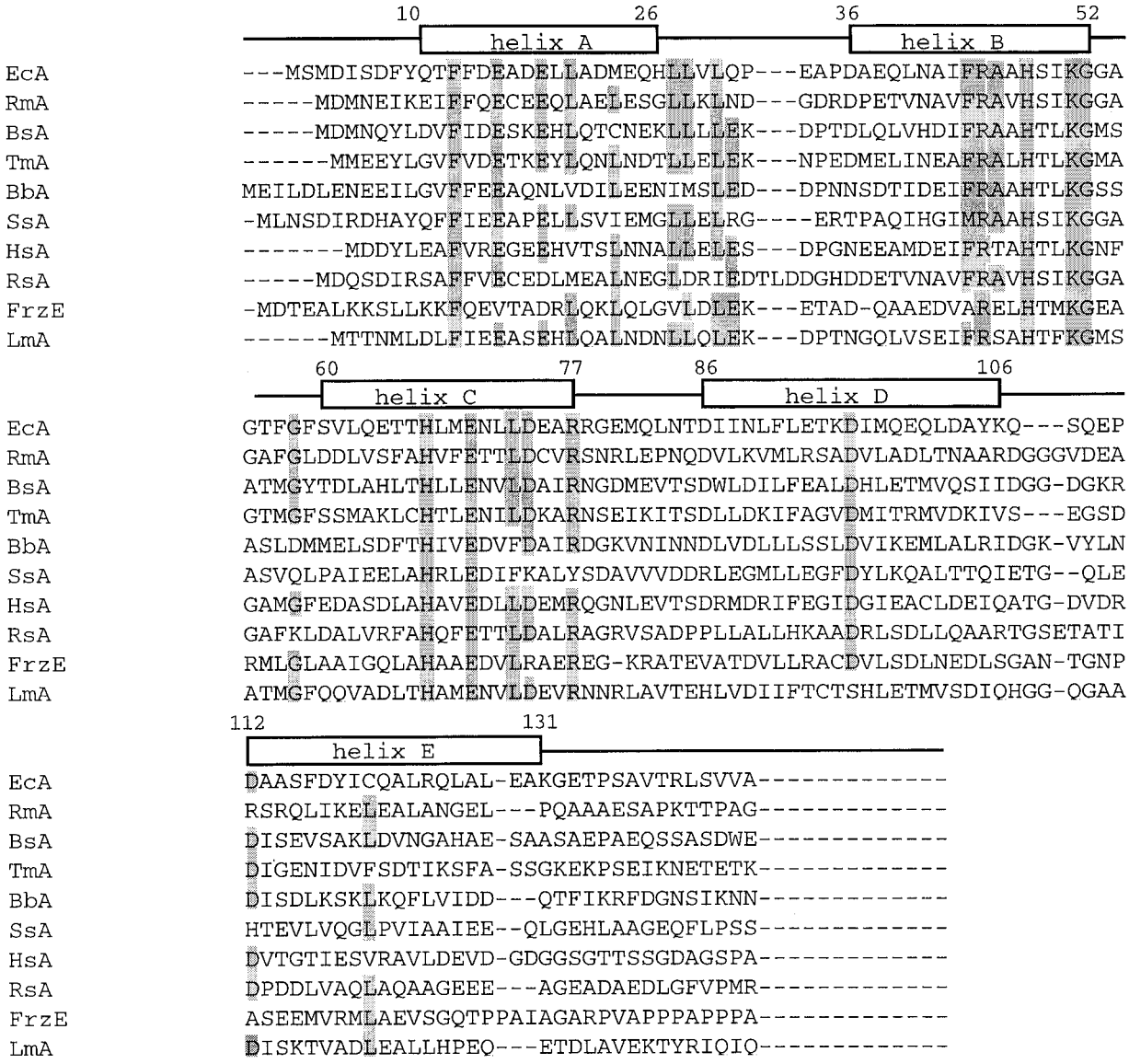

FIGURE 9: Sequence alignment of the phosphotransfer domains of CheA or its homologs from *E. coli* (EcA; Kofoid & Parkinson, 1991), *Rhizobium meliloti* (RmA; Greck et al., 1995), *Bacillus subtilis* (BsA; Fuhrer & Ordal, 1991), *Thermotoga maritima* (TmA; Swanson et al., 1996), *Borrelia burgdorferi* (BbA; G. A. Trueba and R. C. Johnson, unpublished, GenBank entry U28962), *Synechocystis sp.* (SsA; Kaneko et al., 1995), *Halobacterium salinarium* (HsA; Rudolph & Oesterhelt, 1995), *Rhodobacter sphaeroides* (RsA; M. J. Ward, A. W. Bell, and J. P. Armitage, unpublished, GenBank entry S49211), *Myxococcus xanthus* (FrzE; McCleary & Zusman, 1990), and *Listeria monocytogenes* (LmA; Dons et al., 1994). Amino acids that are conserved in seven or more sequences are shaded. The helical regions and residue numbers indicated above the sequences are for *E. coli* CheA. The C-terminal regions of the sequences included in the alignment are domain linkers. The sequences were aligned using the program Clustal W 1.6 (Thompson et al., 1994).

the group which causes the rising edge of the curve of the pH-dependent phosphotransfer rate. The small difference in the pK_a values from our study and the indirect measurement of Conley et al. (1994) may result from different experimental conditions and techniques. The other titratable group remains unidentified and may reside in the kinase domain.

$N^{\delta 1}H$ of His48 is strongly protected from deprotonation likely by hydrogen bonding. The transition from the charged state to neutral states is largely associated with the deprotonation of the $N^{\epsilon 2}H$ nitrogen. Since $N^{\epsilon 2}$ is the site of phosphorylation in the imidazole ring, deprotonation of this nitrogen and stabilization of the $N^{\delta 1}H$ tautomer seem to be critical to the phosphotransfer. The $N^{\delta 1}H$ nitrogen of His48 likely acts as a hydrogen bond donor. There are also indications that $N^{\epsilon 2}$ in the neutral tautomers is also hydrogen-bonded. Due to the low resolution of the current structure of the phosphotransfer domain (Zhou et al., 1995), the hydrogen bond partner(s) of His48 cannot be clearly identified at this stage, although several side chain carboxyl or backbone carbonyl groups are in close proximity with the imidazole ring of His48.

For His67, the pK_a value for $N^{\delta 1}$ higher than those from the carbon-bound ring protons and $N^{\epsilon 2}$ indicates an interesting situation which is not often observed. This phenomenon cannot be easily explained solely by pH-independent tautomerization and fast ring rotation, which result in similar pK_a values for the ring protons and nitrogens. However, the nitrogen chemical shifts at high pH can be well explained by tautomerization, indicating the presence of fast exchange between the tautomers. Therefore, pH-dependent disruption of the tautomerization equilibrium or changes in electronic induction effects on the imidazole atoms may be responsible for the apparent titration differences observed. This situation

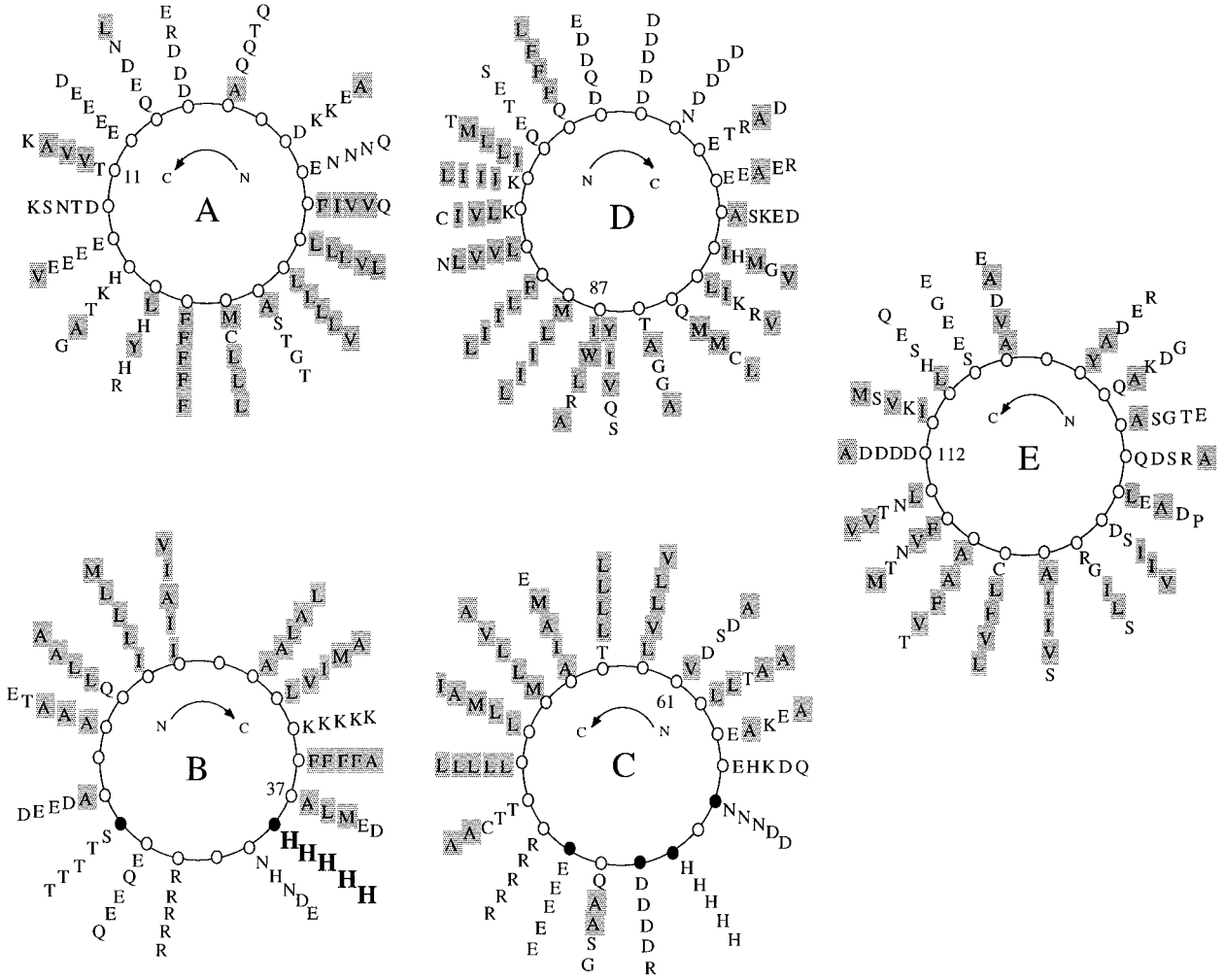

FIGURE 10: Helical wheel diagram of the putative fold of the phosphotransfer domains of the CheA homologs from different organisms. The residues, from inner to outer circles, are for CheA or its homologs from *E. coli*, *B. subtilis*, *T. maritima*, *H. salinarium*, and *M. xanthus*, respectively. The sequence alignment is from Figure 9. Helices A, C, and E are viewed from their C termini, while helices B and D are viewed from their N termini. The positions of helix starts and ends, the relative helix orientations, and the turns joining the helices are based on the general fold of *E. coli* CheA (Zhou et al., 1995). For other CheA homologs, the helices, especially D and E, may need to be rotated to have more favorable hydrophobic interactions. Hydrophobic residues are shaded. Filled circles indicate the residues in *E. coli* CheA that are affected by phosphorylation or titration of His48. The residue numbers inside the helical wheels denote the first N-terminal residues of the helices included in the diagram.

might be caused by pH-dependent changes in interactions between His67 and possibly His48 or other nearby titratable groups. The interactions of His67 with the phosphorylation site were indicated by the slight resonance changes of the His67 imidazole ring upon phosphorylation of His48. These interactions might require that the imidazole ring of His67 have a fairly stable orientation. Fast ring rotation averages different environments and may result in similar titration behavior for the two nitrogens. It is also worth noting that pH-dependent chemical shift changes in a protein are also complicated by additional contributions from structural changes. These changes may not carry a simple pH-dependent property reflecting the pK_a of the imidazole ring under study and also can be localized to a specific atom in the imidazole ring.

The effects of phosphorylation and the mechanisms to stabilize the phosphoryl groups have been studied for other proteins. Localized and small structural changes upon phosphorylation were observed for both the histidine- and serine-phosphorylated forms of the histidine-containing protein (HPr) and the phosphocarrier protein III^{Glc} in the phosphoenolpyruvate:glycose phosphotransferase system (PTS) (Rajagopal et al., 1994; Pullen et al., 1995; Pelton et al., 1993). In HPr, the phosphorylation sites His15 and Ser46 reside in loops joining β-strands and helices. Both residues form the N-caps of the helices. Electrostatic interactions between the helix dipole and the negatively charged phosphoryl group are important for the stabilization of the phosphohistidine or the phosphoserine. The phosphorylation histidine in succinyl-CoA synthetase (SCS) is located in an extended loop (Wolodko et al., 1994). The phosphohistidine is stabilized by interactions with two helix dipoles and a glutamate residue. Having the phosphorylation residue near the N terminus of a helix may be a general motif for proteins capable of phosphorylation. Helix dipole effects also appear to be responsible for the low pK_a values of the unphosphorylated histidines in HPr and III^{Glc}. However, in our case, although the C-terminal position of His48 in $CheA_{1-134}$ is consistent with its relatively high pK_a value, helix dipole effects do not seem to play an important role in stabilizing the phosphohistidine; instead, hydrogen bonding to several residues in helices B and C may contribute the most to the stabilization. These differences suggest a new structural motif at the active site of phosphorylation proteins which

appear to be conserved among the CheA homologs. Additionally, phosphorylation at the $N^{\epsilon 2}$ position rather than at the $N^{\delta 1}$ position also contributes to the stability of the phosphohistidine, since $N^{\delta 1}$-phosphohistidine is more labile than $N^{\epsilon 2}$-phosphohistidine (Hultquist et al., 1966).

Due to the complexity of the chemical and electronic environments and the rigidity of the structure, the amplitudes of chemical shift changes may not directly reflect the extent of the involvement of a residue in interactions with the phosphorylation site. This situation was previously observed in NMR studies of other proteins (Pelton et al., 1993; Pullen et al., 1995). In the phosphotransfer domain of *E. coli* CheA, several positively charged residues in the vicinity of the site of phosphorylation, Arg45, Lys51, Arg77, and Arg78, may also contribute to the stabilization of the phosphohistidine, although phosphorylation did not cause detectable changes in the backbone amide chemical shifts for these residues. Amide chemical shift changes were also not observed for Glu70 which is at the inner interface of helices B and C and is in proximity with His48. However, its interaction with His48 is indicated by the similar apparent pK_a values reported for the Glu70 amide and the His48 imidazole ring. Two highly conserved negatively charged residues Glu70 and Asp74 at the active site would provide otherwise unfavorable interactions with the phosphoryl group, suggesting that a delicate hydrogen bond network is formed to facilitate the phosphotransfer and stabilize the phosphohistidine. The overall small changes in the chemical shifts of the phosphotransfer domain upon phosphorylation indicate that the conformations of the active site residues in the phosphorylated protein closely resemble those in the unphosphorylated form. It is also worth noting that the changes in the amide proton shifts of Ser49, Asn71, and Asp74 upon phosphorylation of His48 are all downfield. Since downfield shift changes of the amide protons are associated with hydrogen bonding (Wagner et al., 1983; Redfield & Papastavros, 1990), the shift changes observed suggest that these amides may interact with the phosphoryl oxygens.

In the histidine kinase CheA and in the phosphocarrier protein III^{Glc} in the PTS pathway of *E. coli* (Pelton et al., 1993), the protonation states before and after phosphorylation and the positions of phosphorylation in the imidazole rings are similar. More discussion of the PTS pathway and its relationship with the chemotaxis system can be found in Hess et al. (1988), Armitage (1993), Lux et al. (1995), and Rowsell et al. (1995). In III^{Glc}, the site of phosphorylation, His90, exists predominantly in the $N^{\delta 1}H$ state in the unphosphorylated protein. The $N^{\delta 1}H$ forms a hydrogen bond with the carbonyl group of Gly92. Upon phosphorylation of His90 $N^{\epsilon 2}$, $N^{\delta 1}$ of this residue remains protonated. A nearby histidine His75 is important for the full function of III^{Glc} and exists predominantly in the $N^{\delta 1}H$ state before and after phosphorylation of His90. His75 also appears to interact with the phosphoryl group. These observations suggest functional or structural roles for His48 and nearby His67 in CheA similar to those for His90 and His75 in III^{Glc}. Interestingly, His67 is totally conserved in all the sequences of CheA homologs examined. However, a mutagenesis study of the functional role of this residue has not been performed. The major difference between the active site histidines in the unphosphorylated CheA and III^{Glc} is that the pK_a value of the phosphorylation site His90 in III^{Glc} is low (<5.0) whereas the pK_a value of His48 in CheA is high (7.8). In addition, the resonances from the $N^{\delta 1}H$ or $N^{\epsilon 2}H$ protons have not been observed for CheA under our experimental conditions. Further detailed comparisons of the two kinases should reveal more mechanistic similarities.

ACKNOWLEDGMENT

We thank Ronald V. Swanson for providing the $CheA_{1-134}$ sample, the *E. coli* strain for the expression of $CheA_{1-233}$, and helpful discussions and Philip Matsumura for providing the full-length CheA protein.

REFERENCES

Armitage, J. P. (1993) in *Signal Transduction−Prokaryotic and Simple Eukaryotic Systems* (Hurjan, J., & Taylor, B. L., Eds.) pp 43−65, Cambridge University Press, Cambridge.

Bachovchin, W. W. (1986) *Biochemistry 25*, 7751−7759.

Barak, R., & Eisenbach, M. (1992) *Biochemistry 31*, 1821−1826.

Bax, A., Ikura, M., Kay, L. E., Torchia, D. A., & Tschudin, R. (1990) *J. Magn. Reson. 86*, 304−318.

Bourret, R. B., Borkovich, K. A., & Simon, M. I. (1991) *Annu. Rev. Biochem. 60*, 401−441.

Conley, M. P., Berg, H. C., Tawa, P., Stewart, R. C., Ellefson, D. D., & Wolfe, A. J. (1994) *J. Bacteriol. 176*, 3870−3877.

Dons, L., Olsen, J. E., & Rasmussen, O. F. (1994) *DNA Sequence 4*, 301−311.

Forman-Kay, J. D., Clore, G. M., & Gronenborn, A. M. (1992) *Biochemistry 31*, 3442−3452.

Fuhrer, D. K., & Ordal, G. W. (1991) *J. Bacteriol. 173*, 7443−7448.

Gegner, J. A., Graham, D. R., Roth, A. F., & Dahlquist, F. W. (1992) *Cell 70*, 975−982.

Greck, M., Platzer, J., Sourjik, V., & Schmitt, R. (1995) *Mol. Microbiol. 15*, 989−1000.

Hess, J. F., Bourret, R. B., & Simon, M. I. (1988) *Nature 336*, 139−143.

Hultquist, D. E., Moyer, R. W., & Boyer, P. D. (1966) *Biochemistry 5*, 322−330.

Kaneko, T., Tanaka, A., Sato, S., Kotani, H., Sazuka, T., Miyajima, N., Sugiura, M., & Tabata, S. (1995) *DNA Res. 2*, 153−166.

Kay, L. E., & Bax, A. (1990) *J. Magn. Reson. 86*, 110−126.

Kihara, M., & Macnab, R. M. (1981) *J. Bacteriol. 145*, 1209−1221.

Kofoid, E. C., & Parkinson, J. S. (1991) *J. Bacteriol. 173*, 2116−2119.

Lupas, A., & Stock, J. (1989) *J. Biol. Chem. 264*, 17337−17342.

Lux, R., Jahreis, K., Bettenbrock, K., Parkinson, J. S., & Lengeler, J. W. (1995) *Proc. Natl. Acad. Sci. U.S.A. 92*, 11583−11587.

Marion, D., Ikura, M., Tschudin, R., & Bax, A. (1989) *J. Magn. Reson. 85*, 393−399.

McCleary, W. R., & Zusman, D. R. (1990) *Proc. Natl. Acad. Sci. U.S.A. 87*, 3898−3902.

Ninfa, E. G., Stock, A., Mowbray, S., & Stock, J. (1991) *J. Biol. Chem. 266*, 9764−9770.

Parkinson, J. S., & Kofoid, E. C. (1992) *Annu. Rev. Genet. 26*, 71−112.

Pelton, J. G., Torchia, D. A., Meadow, N. D., & Roseman, S. (1993) *Protein Sci. 2*, 543−558.

Pullen, K., Rajagopal, P., Branchini, B. R., Huffine, M. E., Reizer, J., Saier, M. H., Scholtz, J. M., & Klevit, R. E. (1995) *Protein Sci. 4*, 2478−2486.

Rajagopal, P., Waygood, E. B., & Klevit, R. E. (1994) *Biochemistry 33*, 15271−15282.

Redfield, A. G., & Papastavros, M. Z. (1990) *Biochemistry 29*, 3509−3514.

Reynolds, W. F., & Tzeng, C. W. (1977) *Can. J. Biochem. 55*, 576−578.

Roman, S. J., Meyers, M., Voltz, K., & Matsumura, P. (1992) *J. Bacteriol. 174*, 6247−6255.

Rowsell, E. H., Smith, J. M., Wolfe, A., & Taylor, B. L. (1995) *J. Bacteriol. 177*, 6011−6014.

Rudolph, J., & Oesterhelt, D. (1995) *EMBO J. 14*, 667−673.

Sanders, D. A., Gillece-Castro, B. L., Stock, A. M., Burlingame, A. L., & Koshland, D. E., Jr. (1989) *J. Biol. Chem. 264*, 21770−21778.
Schuster, I. I., & Roberts, J. D. (1979) *J. Org. Chem. 44*, 3864−3867.
Simms, S. A., Stock, A. M., & Stock, J. B. (1985) *J. Biol. Chem. 260*, 10161−10168.
Slonczewski, J. L., Macnab, R. M., Alger, J. R., & Castle, A. M. (1982) *J. Bacteriol. 152*, 384−399.
Stewart, R. C., & Dahlquist, F. W. (1987) *Chem. Rev. 87*, 997−1025.
Stock, A. M., Wylie, D. C., Mottonen, J. M., Lupas, A. N., Ninfa, E. G., Ninfa, A. J., Schutt, C. E., & Stock, J. B. (1988a) *Cold Spring Harbor Symp. Quant. Biol. 53*, 49−57.
Stock, A. M., Chen, T., Welsh, D., & Stock, J. B. (1988b) *Proc. Natl. Acad. Sci. U.S.A. 85*, 1403−1407.
Stock, J. B., Ninfa, A. J., & Stock, A. M. (1989) *Microbiol. Rev. 53*, 450−490.
Swanson, R. V., Schuster, S. C., & Simon, M. I. (1993) *Biochemistry 32*, 7623−7629.
Swanson, R. V., Sanna, M. G., & Simon, M. I. (1996) *J. Bacteriol. 178*, 484−489.
Thompson, J. D., Higgins, D. G., & Gibson, T. J. (1994) *Nucleic Acids Res. 22*, 4673−4680.
van Dijk, A. A., de Lange, L. C. M., Bachovchin, W. W., & Robillard, G. T. (1990) *Biochemistry 29*, 8164−8171.
van Dijk, A. A., Scheek, R. M., Dijkstra, K., Wolters, G. K., & Robillard, G. T. (1992) *Biochemistry 31*, 9063−9072.
Wagner, G., Pardi, A., & Wüthrich, K. (1983) *J. Am. Chem. Soc. 105*, 5948−5949.
Witanowski, M., Stefaniak, L., Januszewsiki, H., Grabowski, Z., & Webb, G. A. (1972) *Tetrahedron 28*, 637−653.
Wolodko, W. T., Fraser, M. E., James, M. N. G., & Bridger, W. A. (1994) *J. Biol. Chem. 269*, 10883−10890.
Worley, K. C., Wiese, B. A., & Smith, R. F. (1995) *Genome Res. 5*, 173−184.
Zhou, H., Lowry, D. F., Swanson, R. V., Simon, M. I., & Dahlquist, F. W. (1995) *Biochemistry 34*, 13856−13870.
Zhou, H., McEvoy, M. M., Lowry, D. F., Swanson, R. V., Simon, M. I., & Dahlquist, F. W. (1996) *Biochemistry 35*, 433−443.
Zuiderweg, E. R. P. (1990) *J. Magn. Reson. 86*, 346−357.

BI961663P